Plant Biotechnology 27, 401–408 (2010)

Original Paper

Arabidopsis CFD is an ortholog of *Chlamydomonas* Ccs1 that is required for *c*-type heme assembly in chloroplasts

Tsuneaki Takami[1,2], Yoshichika Kobayashi[1], Toshiharu Shikanai[2,*]

[1] Graduate School of Agriculture, Kyushu University, Fukuoka 812-8581, Japan;
[2] Department of Botany, Graduate School of Science, Kyoto University, Kyoto 606-8502, Japan
* E-mail: shikanai@pmg.bot.kyoto-u.ac.jp Tel: +81-75-753-4247 Fax: +81-75-753-4257

Received May 13, 2010; accepted June 14, 2010 (Edited by J. Yamaguchi)

Abstract The *Arabidopsis thaliana cfd* (*cytochrome f deficient*) mutant was isolated by the sensitivity of its photosystem II to low temperature using a chlorophyll fluorescence imaging technique. The *cfd* mutant is defective in intersystem electron transport even at 23°C, secondarily leading to photodamage of PSII at 4°C. Map-based cloning revealed that the *cfd* phenotype is due to a mutation in *At1g49380*, which encodes a putative plastid-targeting protein with high similarity to Ccs1 in *Chlamydomonas reinhardtii*. Ccs1 is required for *c*-type cytochrome (Cyt) assembly in chloroplasts. Consistent with the high sequence similarity of *At1g49380* and Ccs1, the levels of Cyt *f* heme and Cyt *f* were low in the *cfd* mutant. We conclude that CFD is an ortholog of *Chlamydomonas* Ccs1. *In vitro* ferredoxin-dependent plastoquinone reduction activity was not affected in *cfd*, suggesting that system II *c*-type Cyt biogenesis is required for the machinery of photosystem I cyclic electron transport.

Key words: *Arabidopsis*, chloroplast, cytochrome *f*, heme, PSI cyclic electron transport.

The light reactions of photosynthesis are electron transport in thylakoid membranes, and the electron transport is mediated by three protein complexes, photosystem (PS) II, PSI and cytochrome (Cyt) b_6f. Electrons excised from water in PSII are finally transferred to $NADP^+$ via Cyt b_6f and PSI. This linear electron transport is coupled with proton translocation across the thylakoid membranes, and the resulting ΔpH is utilized in ATP synthesis. In contrast, PSI cyclic electron transport is mediated solely by PSI and generates ATP without accumulating NADPH (Shikanai 2007). In *Arabidopsis thaliana*, PSI cyclic electron transport consists of two partly redundant routes taken by electrons, the PGR5 (PROTON GRADIENT REGULATION 5)-dependent and NAD(P)H dehydrogenase (NDH)-dependent pathways (Munekage et al. 2004).

The protein complexes in thylakoid membranes consist of both nuclear- and plastid-encoded subunits and also prosthetic groups. The assembly of functional complexes requires multiple steps, including concerted gene expression in two genomes, stoichiometric synthesis of subunits, stepwise assembly of the complex, and ligation of a number of various cofactors (Rochaix, 2004). Recently, the assembly processes were studied using mutants specifically defective in each step. Both LPA1 (LOW PSII ACCUMULATION) and LPA2 were identified in *Arabidopsis* mutants defective in PSII accumulation (Ma et al. 2007; Peng et al. 2006). While LPA1 is likely to be a chaperone that is required for the efficient assembly of the PSII reaction center, LPA2 is involved in the assembly of CP43 into PSII. In contrast, Ycf4 was identified in knockout lines of the plastid *ycf4* gene in *Chlamydomonas reinhardtii* (Boudreau et al. 1997), and the protein complex containing Ycf4 was shown to be a scaffold for PSI assembly (Ozawa et al. 2009).

The Cyt b_6f complex consists of four large subunits (Cyt *f*, Cyt b_6, subunit IV, and the Rieske subunit) and four small subunits (PetG, PetL, PetM, and PetN) (Whitelegge et al. 2002). To orchestrate the assembly of this multi-subunit complex, the synthesis of certain plastid-encoded subunits is downregulated by the absence of other subunits in the same complex (Wollman et al. 1999). In this regulatory process known as CES (control by epistasy of synthesis), the translation of *petA* (encoding Cyt *f*) is impaired in a Δ*petD* strain of *Chlamydomonas* (Choquet et al. 1998). A similar story is also true in the flowering plant maize, where *petA* translation is impaired in *crp1* (*chloroplast RNA processing 1*) mutants, which are defective in the expression of *petD* encoding subunit IV (Barkan et al.

Abbreviations: CES, control by epistasy of synthesis; Cyt, cytochrome; Fd, ferredoxin; PQ, plastoquinone; PS, photosystem;
This article can be found at http://www.jspcmb.jp/

1994). Two heme prosthetic groups are covalently bound to the Cyt b_6f subunits: heme *c* of Cyt *f* and heme c_i of Cyt b_6 (Kurisu et al. 2003). The assembly of *c*-type Cyt is mediated by at least three distinct systems (I, II and III) observed in different organisms and different subcellular locations (Kranz et al. 2009). Cyt *f* assembly depends on system II, which occurs in chloroplasts and some bacteria such as cyanobacteria. Genetic studies using *Chlamydomonas* have identified six loci, plastid *ccsA* and nuclear *CCS1-CCS5*, involved in the maturation of chloroplast *c*-type Cyt (Dreyfuss et al. 2003; Hamel et al. 2003). However, it has been suggested that the assembly of heme c_i in Cyt b_6 requires a distinct system (Kuras et al. 2007).

In this study, we characterized an *Arabidopsis cfd* (*cytochrome f deficient*) mutant defective in Cyt *f* assembly that was originally isolated as a low-temperature sensitive mutant. The *cfd* mutant has one amino acid alteration in *At1g49380*, which encodes an ortholog of Ccs1 in *Chlamydomonas*.

Materials and methods

Plant materials and culture conditions

Arabidopsis thaliana (ecotype Columbia *gl1*) used in this work was grown in soil under growth chamber conditions (50 μmol photons $m^{-2}s^{-1}$, 16-h photoperiod, 23°C). Three to four weeks after germination, plants were used for experiments.

Chlorophyll fluorescence and P700 analysis

Chlorophyll fluorescence images were captured by FluorCAM 700MF (PSI, Brno, Czech). Chlorophyll fluorescence was measured using a MINI-PAM portable chlorophyll fluorometer (Walz, Effeltrich, Germany). Φ_{PSII} was calculated as $(Fm' - Fs)/Fm'$, where Fm' is the maximum fluorescence level in the light, and *Fs* is the steady-state fluorescence level. ETR (electron transport rate) was calculated as Φ_{PSII} x photon flux density (μmol photons $m^{-2}s^{-1}$). NPQ (nonphotochemical quenching of chlorophyll fluorescence) was calculated as $(Fm-Fm')/Fm'$. qL was calculated as $\{\Phi_{PSII}\text{light}/(1-\Phi_{PSII}\text{light})\}\times\{(1-Fv/Fm)/(Fv/Fm)\}\times(\text{NPQ}+1)$ (Miyake et al. 2009). The redox change of P700 was assessed by monitoring absorbance at 810 nm using a PAM chlorophyll fluorometer equipped with an ED P700DW emitter-detector unit (Walz, Effeltrich, Germany) as described previously (Munekage et al. 2002).

Map-based cloning

The *cfd* mutation was mapped using molecular markers based on cleaved amplified polymorphic sequences (Konieczny and Ausubel 1993) and simple sequence length polymorphisms (Bell and Ecker 1994). Genomic DNA was isolated from F_2 plants derived from a cross between *cfd* (genetic background of Columbia *gl1*) and the wild type (Landsberg *erecta*). Homozygous F_2 plants (*cfd*/*cfd*) exhibiting the low *Fv*/*Fm* phenotype after chilling treatment (continuous light of 50 μmol photons $m^{-2}s^{-1}$ at 4°C for one week) were selected. *At1g49380* was amplified by PCR using Ex Taq DNA polymerase (Takara, Kyoto, Japan) using the genomic DNA of the wild type and *cfd*. The PCR products were directly sequenced using a dye terminator cycle sequencing kit and an ABI prism 3100 sequencer (Applied Biosystems, CA, USA). The primer sequences for the markers are listed in Table 2. After PCR, the fragments amplified by T18C15 were digested with *Hin*dIII.

For complementation of the *cfd* mutation, the wild-type genomic sequence including *At1g49380* was amplified (from 5′-CTAATACTAAGGCTAATTACGAG-3′ to 5′-GAAACTTC-ACTCAGCACTCTC-3′). The PCR product was subcloned into pBIN19. The resulting plasmid was introduced into the *Agrobacterium tumefaciens* C58C1 strain and the bacteria were used to transform homozygous *cfd* plants by floral dipping (Clough and Bent 1998).

Protein analysis

For immunoblot analysis, thylakoid proteins were loaded onto SDS-PAGE on an equal chlorophyll basis. The signals were detected using an ECL Plus Western Blotting Detection Kit (GE Healthcare UK Ltd, Buckinghamshire, UK) and visualized by a LAS3000 chemiluminescence analyzer (Fuji Film, Tokyo, Japan). Cyt *f* heme was detected by peroxidase activity (Vargas et al. 1993). The presented results are representative of three independent experiments.

RNA gel blot analysis

For RNA gel blot analysis, total RNA was isolated from the rosette leaves of wild type and *cfd* using sepasol RNA I super (Nacalai Tesque, Kyoto, Japan). Five μg of RNA was loaded onto a denaturing formaldehyde gel, transferred to positive-charged nylon membranes, and hybridized with gene-specific DIG (Roche Diagnostics, Switzerland) labeled probes. The sequences of the PCR primers used for probe preparation are listed in Table 2. The signals were detected using CDP-*Star* Detection Reagent (GE Healthcare UK Ltd, Buckinghamshire, UK) and captured by Hyperfilm ECL (GE Healthcare UK Ltd, Buckinghamshire, UK).

Analysis of PSI cyclic electron transport

Ferredoxin (Fd)-dependent plastoquinone (PQ) reduction activity was measured in ruptured chloroplasts as previously described (Munekage et al. 2002). As electron donors, 5 μM maize Fd and 0.25 mM NADPH were used.

Results and discussion

The cfd mutant is defective in intersystem electron transport

The *Arabidopsis cfd* (*cytochrome f deficient*) mutant was identified based on the sensitivity of its PSII to low temperature using a chlorophyll fluorescence imaging technique (Figure 1; Takami et al. manuscript submitted). The chlorophyll fluorescence parameter *Fv*/*Fm* reflects the maximum activity of PSII. Although *Fv*/*Fm* was comparable between *cfd* and wild-type plants at 23°C, it was much reduced in *cfd* plants when seedlings were exposed to low temperature (4°C) for

Table 1. Maximum activity of PSII (*Fv/Fm*) in wild type and *cfd* before and after chilling treatment

	WT	*cfd*	*cfd*+*CFD*
Fv/Fm			
Control	0.765 ± 0.008	0.741 ± 0.014	0.760 ± 0.005
Chilling treatment.	0.744 ± 0.007	0.618 ± 0.030	0.723 ± 0.017

After chilling treatment (continuous light 50 μmol photons m^{-2} s^{-1}, 4°C for 1 week), plants were dark adapted for 1h at room temperature before the *Fv/Fm* measurement. Means ± standard deviation (n = 5–6).

Table 2. Sequences of primers

T1N15-F	5′-GAACCGAACCTAATATCGGATC-3′	mapping
T1N15-R	5′-CCGATCTTCACTATTATTTTGCC-3′	mapping
T18C15-F	5′-GTTGGGACGACGTTCAATGAG-3′	mapping
T18C15-R	5′-CTAGGTTCATCTCCAGAGAAAG-3′	mapping
petA-F	5′-CAGATTTATCCTGATGGTAGC-3′	*petA* probe
petA-R	5′-TTGTGCCAAAACAACCGATCC-3′	*petA* probe
petB-F	5′-CACGTATTTCGTGTATACCTC-3′	*petB* probe
petB-R	5′-GACCAGAAATACCTTGCTTAC-3′	*petB* probe
petC-F	5′-CGAAGATGAATCATCAAATGG-3′	*petC* probe
petC-R	5′-TAATCCTTGGGTCAAGGTTCG-3′	*petC* probe
petD-F	5′-TATTCTTGGTACCATTGCCTG-3′	*petD* probe
petD-R	5′-ATCAATCGGTAATGTTGCTCC-3′	*petD* probe

seven days (Table 1). This result suggests that PSII of *cfd* is sensitive to low temperature.

In addition to the sensitivity of PSII to low temperature, the growth rate of *cfd* was mildly reduced even at 23°C relative to wild type (Figure 1). Even though the maximum activity of PSII is not affected at 23°C in *cfd*, photosynthetic electron transport could still be partially impaired. To test this possibility, the light-intensity dependence of ETR and NPQ were compared between *cfd* and wild-type plants cultured at 23°C (Figure 2A, B). While ETR reflects the relative rate of electron transport through PSII during steady-state photosynthesis, NPQ is mainly caused by thermal

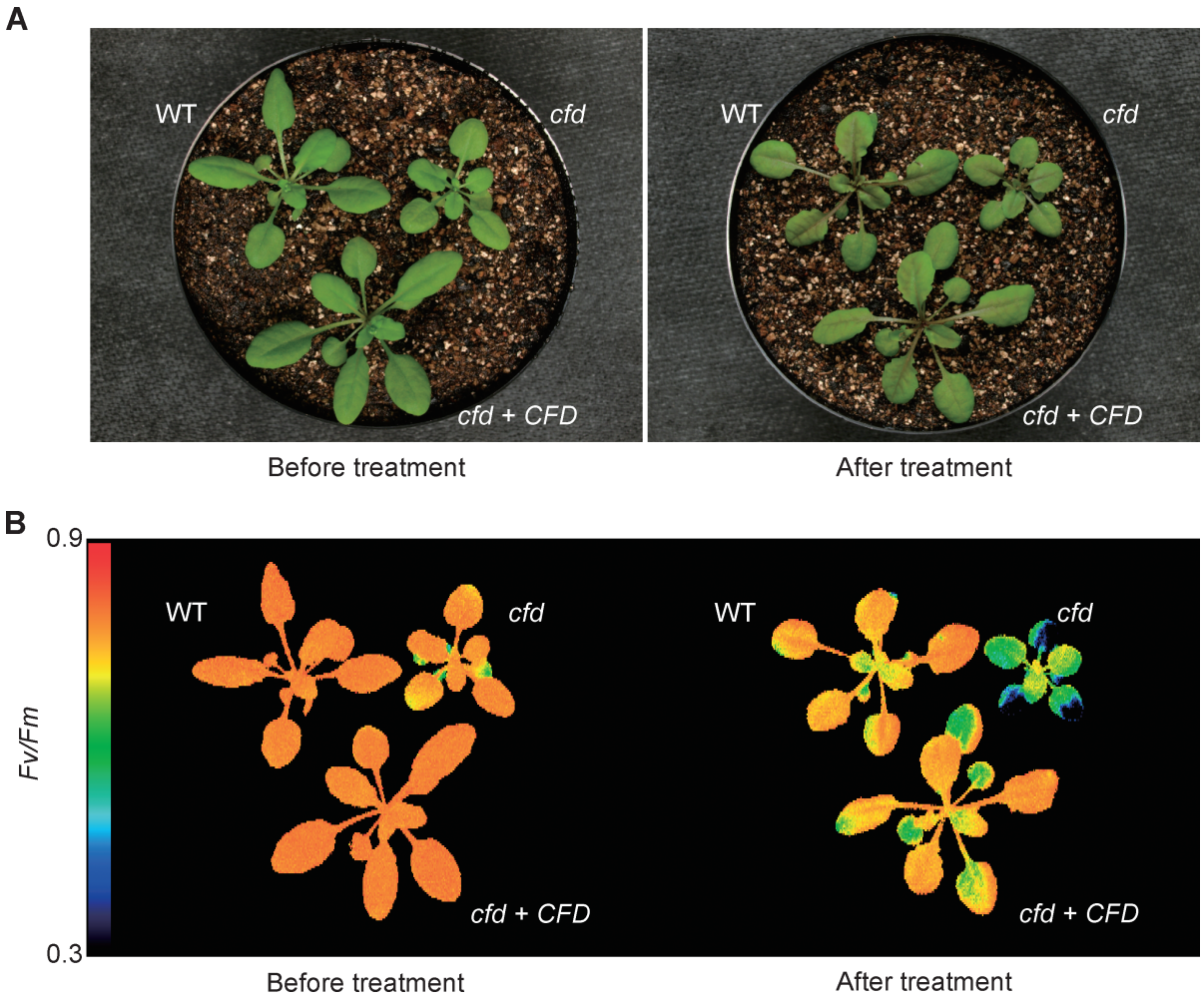

Figure 1. Visible phenotype of the *cfd* mutant. (A) Wild-type (WT) and *cfd* seedlings before and after chilling treatment (continuous light of 50 μmol photons m^{-2} s^{-1} at 4°C for one week). (B) Detection of chilling sensitivity by chlorophyll fluorescence imaging. Images represent the maximum activity of PSII (*Fv/Fm*). *cfd*+*CFD*: *cfd* transformed with the wild-type genomic *CFD* gene.

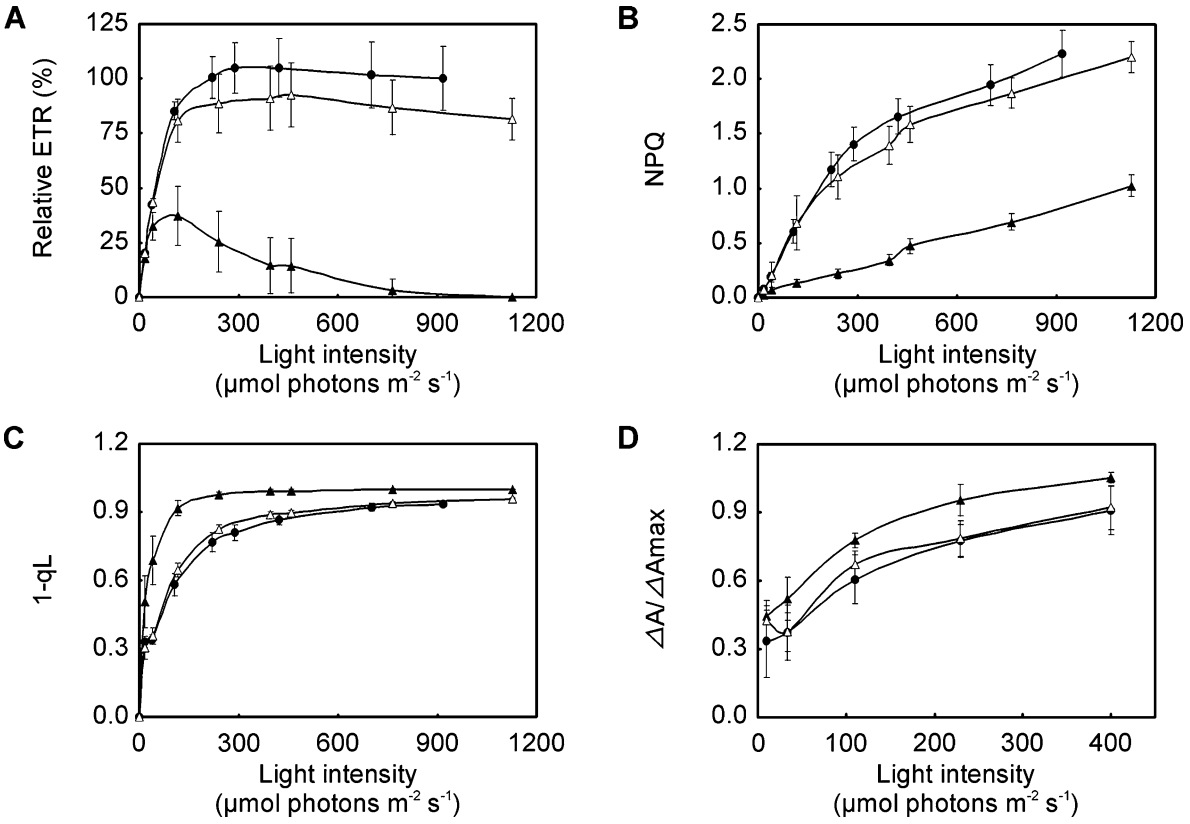

Figure 2. *In vivo* analysis of photosynthetic electron transport. (A) Light-intensity dependence of the relative electron transport rate (ETR). ETR was calculated as Φ_{PSII} x light intensity (μmol photons m^{-2} s^{-1}) and is presented relative to the maximum wild-type ETR (100%). (B) Light-intensity dependence of NPQ. (C) Light-intensity dependence of 1-qL reflecting the Q_A reduction state. (D) Light-intensity dependence of the P700 oxidation ratio (ΔA/ΔAmax). Closed circles, wild-type; closed triangles, *cfd*; open triangles, *cfd*+*CFD*. Each value represents the mean±standard deviation; in (A)–(C), (n=5–6); in (D), (n=4−5).

dissipation of absorbed excess light energy in flowering plants, which depends on the buildup of ΔpH across the thylakoid membrane (Krause and Weis 1991). Even at 23°C, both ETR and NPQ were severely affected at low-light intensities in *cfd* (Figure 2A, B), consistent with the growth phenotype (Figure 1). This result implies that the sensitivity of PSII to low temperature is secondarily caused by the primary defect in photosynthetic electron transport.

To characterize the possible defect in photosynthetic electron transport in *cfd*, the redox levels of both photosystems were determined during steady-state photosynthesis (Figure 2C, D). The 1-qL parameter reflects the reduction state of the quinone acceptor of PSII (Q_A) (Kramer et al. 2004; Miyake et al. 2009), and it was less oxidized in *cfd* than in wild type (Figure 2C). This result suggests that electron transport is restricted downstream of the Q_A site of PSII. The ΔA/ΔAmax parameter indicates the oxidation state of the special pair of reaction center chlorophylls in PSI (P700). In wild type, P700 is more oxidized under higher light intensity probably due to the downregulation PSII photochemistry by NPQ and the restriction of electron transport at the Cyt b_6f complex. Despite the defect in NPQ in *cfd* (Figure 2B), P700 was more oxidized than in wild type except at very low light intensity (Figure 2D). This result suggests that electron transport is more severely impaired before P700 in *cfd* than in wild type. This phenotype is similar to that of *pgr1* (*proton gradient regulation 1*), which are conditionally defective in the activity of the Cyt b_6f complex (Munekage et al. 2001), and of *paa1* (*p-type ATPase in Arabidopsis*), which are partially defective at accumulating plastocyanin (Shikanai et al. 2003). Based on all the electron transport analysis results (Figure 2), electron transport in *cfd* is likely to be limited in the intersystem between Q_A of PSII and P700 of PSI, possibly at PQ, the Cyt b_6f complex or plastocyanin.

The cfd mutation maps to a gene encoding a Chlamydomonas Ccs1 homolog

The *cfd* phenotype was found to be recessive and due to a defect in a single gene (data not shown). Therefore, the gene was identified by map-based cloning. A *cfd* mutant (Columbia *gl1* background) was crossed with a polymorphic wild-type strain (Landsberg *erecta*). Analysis of 164 F_2 plants resulted in the identification of a 574-kb region surrounded by the molecular markers

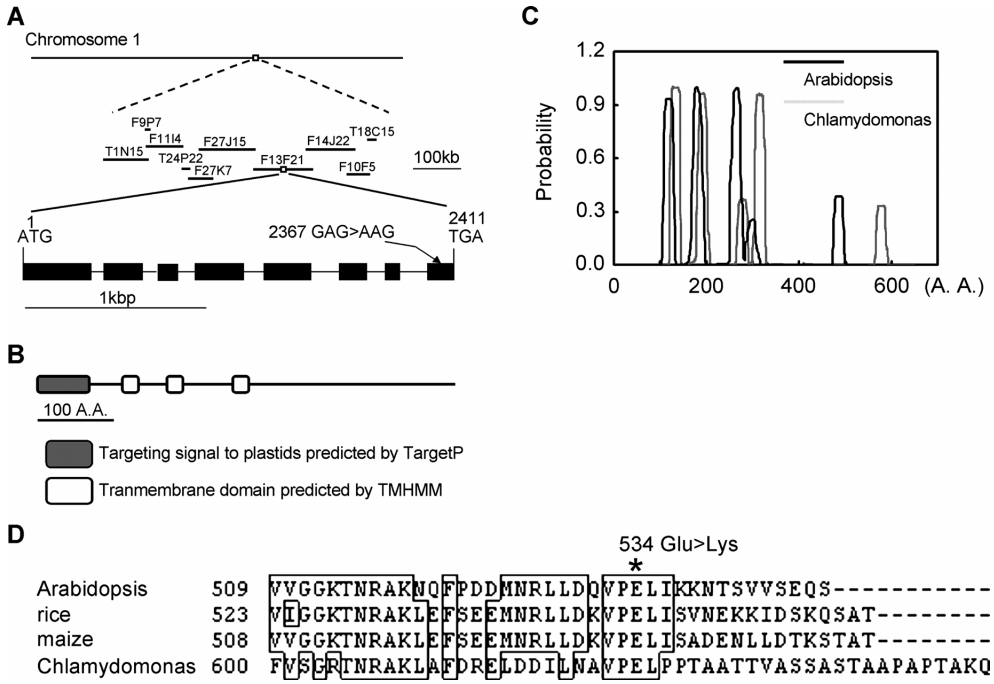

Figure 3. *cfd* is defective in an ortholog of Chlamydomonas *Ccs1*. (A) The *cfd* mutation was mapped between the molecular markers T1N15 and T18C15 on chromosome 1. The *cfd* mutation (G to A) was finally identified in the fifth exon of *At1g49380*, and it changes Glu^{534} to Lys. The black boxes stand for exons. (B) A plastid targeting signal and transmembrane domains predicted by the TargetP and TMHMM programs, respectively. (C) Comparison of transmembrane regions between *Arabidopsis* CFD/AtCcs1 and *Chlamydomonas* Ccs1 as predicted by TMHMM. (D) Alignment of the C-terminal region of CFD, including the Glu^{534} affected in *cfd*.

T1N15 and T18C15 in the middle of chromosome 1. The genomic sequences of 23 genes predicted to encode plastid-targeted proteins (predicted by TargetP. http://www.cbs.dtu.dk/services/TargetP/) were determined, and a sequence alteration was found in a single gene, *At1g49380*.

At1g49380 consists of eight exons and seven introns (Figure 3A). The nucleotide alteration was found in the last exon, and it results in an amino acid alteration from glutamate^{534} (GAG) to lysine (AAG). To verify that the *cfd* phenotype was due to the mutation in *At1g49380*, its wild-type genomic sequence (see Materials and methods for detail) was introduced into *cfd*. This complementation fully suppressed the high chlorophyll fluorescence, electron transport, and growth phenotypes at 23°C, and also the sensitivity of PSII to low temperature in three independent transformants (Figure 1). We conclude that the *cfd* defect is due to the mutation in *At1g49380* (*CFD*).

The *CFD* gene encodes a putative protein composed of 547 amino acids and is a single copy gene in *Arabidopsis*. TargetP predicted that the putative CFD protein targets to plastids and the first 69 amino acids are the targeting signal to plastids (Figure 3B). The predicted amino acid sequence of its mature form shows high similarity (44.9% amino acid identity in the predicted mature protein) with the Ccs1 protein, which is involved in Cyt *c* biogenesis in *Chlamydomonas* (Dreyfuss et al. 2003), suggesting that the *CFD* gene encodes the *Arabidopsis* ortholog of *Ccs1*. The TMHMM (http://www.cbs.dtu.dk/services/TMHMM/) program predicted that CFD contains three transmembrane domains, as in *Chlamydomonas* Ccs1 (Figure 3B, C). Genes with high similarity to *CFD* are also conserved in flowering plants, including rice and maize (Figure 3D). Based on the topology of Ccs1 (Dreyfuss et al. 2003), the *cfd* mutation alters a well-conserved glutamate in the C-terminal tail exposed to the thylakoid lumen.

The cfd mutant is partially defective at accumulating the Cyt b_6f complex

Chlamydomonas Ccs1 is involved in system II of Cyt *c* biogenesis and its mutant is defective at accumulating Cyt *f* in the Cyt b_6f complex and Cyt c_6, which functions in electron transport between the Cyt b_6f complex and PSI (Dreyfuss et al. 2003). To test the possibility that *Arabidopsis* CFD is orthologous to *Chlamydomonas* Ccs1, we compared the level of Cyt *f* between *cfd* and wild type. In *cfd* plants cultured at 23°C, the Cyt *f* level was reduced to 25–50% of the wild-type level, but other photosynthetic proteins (PsaA, PsbB and PsbS) were not significantly affected (Figure 4). To study the accumulation of Cyt *f* in thylakoids further, Cyt *f* heme was detected by peroxidase activity of the heme group in Cyt *f* using the ECL reagent as a substrate for a luminol reaction (Vargas et al. 1993). Consistent with the protein

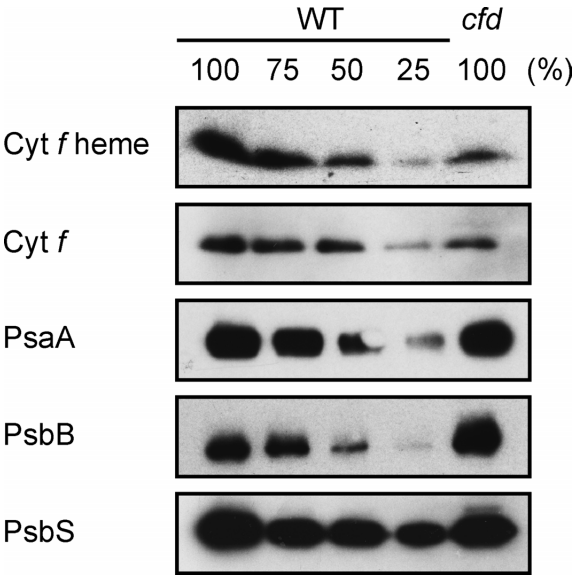

Figure 4. Heme-staining and protein blot analysis of thylakoid membrane proteins. Heme groups in Cyt *f* were detected by peroxidase activity. Immunodetection of Cyt *f*, PsaA (reaction center of PSI), PsbB (CP47, PSII subunit) and PsbS (CP22, PSII subunit). Thylakoid membrane proteins were prepared from seedlings cultured at 23°C. Samples were loaded on a chlorophyll basis (0.5 μg for 100%) and a dilution series was performed as indicated.

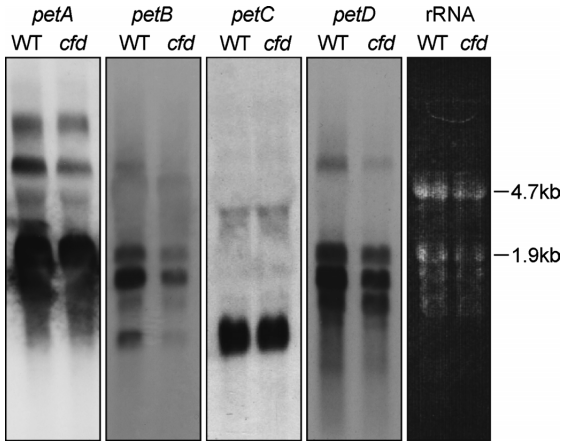

Figure 5. RNA gel blot analysis of subunit genes of the Cyt b_6f complex. Transcripts of plastid-encoded *petA* (Cyt *f*), *petB* (Cyt b_6), *petD* (subunit IV), and nucleus-encoded *petC* (Rieske subunit) were compared between wild type (WT) and *cfd*. Samples were loaded on an equal total RNA basis (5 μg). rRNA was used as a loading control. The size of RNA was estimated by the position of rRNA.

blot analysis, the Cyt *f* heme level was again reduced to 25-50% of the wild-type level.

The Cyt *f* apoprotein is encoded by the plastid *petA* gene in *Arabidopsis*. To test the possibility that Cyt *f* accumulation is restricted at the gene expression level, *cfd* and wild type were analyzed by RNA gel blot. We did not detect any difference in *petA* transcript levels between *cfd* and wild type (Figure 5). Two additional plastid genes, *petB* and *petD*, encode core subunits of the Cyt b_6f complex, Cyt b_6 and Subunit IV respectively, while the nuclear *petC* gene encodes the Rieske iron-sulfur subunit. Neither the levels nor the patterns of *petC* were affected in *cfd*, although the levels of *petB* and *petD* transcripts were slightly lower compared to wild type (Figure 5). Downregulation of subunit synthesis is induced by a primary defect in the synthesis of another subunit of the same protein complex (the CES process). In the case of the Cyt b_6f complex, if the primary defect is in the synthesis of subunit IV, Cyt *f* synthesis is impaired (Choquet et al. 1998). *cfd* is likely to be defective in the process of heme attachment to Cyt *f* apoprotein, as the transcript levels of subunits of the Cyt b_6f complex were not affected (Figure 5). Based on these results, the reduction in Cyt *f* accumulation was not caused by CES, although we do not eliminate the possibility that *petB* and *petD* transcript levels are secondarily regulated via low Cyt *f* level (Figure 5). All the results support the idea that Cyt *f* biogenesis, most probably the attachment of *c*-type heme to Cyt *f*, limits the accumulation of Cyt *f* in *cfd*. We conclude that *Arabidopsis* CFD is an ortholog of *Chlamydomonas* Ccs1. Consequently, it would be simpler if we renamed the *cfd* mutant *ccs1*, but the name "CCS1" was already used for a Cu chaperone for superoxide dismutase in *Arabidopsis* (Winz and Vulpe 2002). To avoid any confusion, we kept using *cfd* for the mutant and have referred to the protein as CFD/AtCcs1 in this manuscript.

Ccs1 is also required for the biogenesis of Cyt c_6 in *Chlamydomonas* (Dreyfuss et al. 2003), suggesting that CFD/AtCcs1 is also involved in the same process. However, Cyt c_6 does not function in intersystem electron transport, and its mutant phenotype would be too subtle to evaluate its function in *cfd* (Gupta et al. 2002). A specific antibody against *Arabidopsis* Cyt c_6 is not available at present. Although we could not test it experimentally, it is probable that CFD/AtCcs1 is required for the biogenesis of Cyt c_6 in *Arabidopsis*.

c-type heme biogenesis is not essential for PSI cyclic electron transport

The *cfd* mutant is partially defective in *c*-type Cyt biogenesis, and the mutant can grow photoautotrophically. This enabled us to test whether *c*-type Cyt biogenesis is required for PSI cyclic electron transport. In flowering plants, PSI cyclic electron transport consists of two partly redundant pathways: a PGR5-dependent, antimycin A-sensitive pathway is the main route, and a minor pathway depends on the chloroplast NDH complex (Munekage et al. 2004; Munekage and Shikanai 2005; Shikanai 2007). The components of these electron transport systems are still unclear, especially in the PGR5-dependent route, although they may include *c*-type Cyt. To test this possibility, the activity of Fd-dependent PQ reduction,

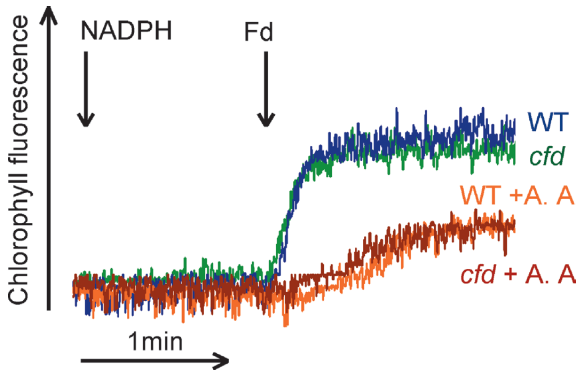

Figure 6. Fd-dependent PQ reduction activity in ruptured chloroplasts. Ruptured chloroplasts were isolated from wild-type and *cfd* leaves (10 μg of chlorophyll ml^{-1}). Electron donation to PQ was monitored as the increase in chlorophyll fluorescence by addition of 0.25 mM NADPH and 5 μM Fd under weak illumination (1 μmol photons m^{-2} s^{-1}). To inhibit PGR5-dependent PQ reduction, 10 μM antimycin A (A. A) was added prior to analysis. The fluorescence level was standardized by the F_m level.

which mediates PSI cyclic electron transport *in vivo*, was compared between *cfd* and wild type using a ruptured chloroplast system. In this assay, addition of NADPH is required to reduce Fd via a reverse FNR reaction (Fd-dependent NADP$^+$ reductase) in the dark (Miyake and Asada 1994). PQ reduction is monitored as an increase in chlorophyll fluorescence emitted from PSII (Endo et al. 1998).

By adding Fd, the PQ pool was reduced via two pathways of PSI cyclic electron transport. As reported previously (Munekage et al. 2004; Okegawa et al. 2008; Peng et al. 2009), addition of antimycin A specifically inhibits PGR5-dependent PQ reduction, and the remaining activity depends on the chloroplast NDH complex. PQ reduction was not affected in the presence or absence of antimycin A (Figure 6). This result suggests that neither PGR5-dependent nor NDH-dependent PSI cyclic activity is affected in *cfd*. This result is consistent with the fact that PSI cyclic activity is not affected in *pgr1*, which is conditionally defective in the activity of the Cyt b_6f complex (Okegawa et al. 2005), or mutants defective in the dimmer formation of the complex (Schwenkert et al. 2007). However, we do not eliminate the possibility that our *in vitro* PSI cyclic assay does not quantitatively reflect the *in vivo* rate of the electron transport and that the low level of *c*-type Cyt does not limit the electron transport in our system. In contrast to *pgr5* (Munekage et al. 2002), however, P700 is more oxidized in the light in *cfd* (Figure 2D), suggesting that the balance between linear and PSI cyclic electron transport was not affected in *cfd*.

Acknowledgements

We thank A. Makino and K.K. Niyogi for their gifts of the Cyt *f* and PsbS antibodies. This work was supported by the Ministry of Education, Culture, Sports, Science, and Technology of Japan (22114509 to TS); Genomics for Agricultural Innovation (the Ministry of Agriculture, Forestry, and Fisheries of Japan, GPN0008 to TS); and Scientific Research for Plant Graduate Student from Nara Institute of Science and Technology (The Ministry of Education, Culture, Sports, Science and Technology to TT).

References

Barkan A, Walker M, Nolasco M, Johnson D (1994) A nuclear mutation in maize blocks the processing and translation of several chloroplast mRNAs and provides evidence for the differential translation of alternative mRNA forms. *EMBO J* 13: 3170–3181

Bell CJ, Ecker JR (1994) Assignment of 30 microsatellite loci to the linkage map of *Arabidopsis*. *Genomics* 19: 137–144

Boudreau E, Takahashi Y, Lemieux C, Turmel M, Rochaix J-D (1997) The chloroplast *ycf3* and *ycf4* open reading frames of *Chlamydomonas reinhardtii* are required for the accumulation of the photosystem I complex. *EMBO J* 16: 6095–6104

Choquet Y, Stern DB, Wostrikoff K, Kuras R, Girard-Bascou J, Wollman FA (1998) Translation of cytochrome *f* is autoregulated through the 5′ untranslated region of *petA* mRNA in *Chlamydomonas* chloroplasts. *Proc Natl Acad Sci USA* 95: 4380–4385

Clough SJ, Bent AF (1998) Floral dip: A simplified method for *Agrobacterium*-mediated transformation of *Arabidopsis thaliana*. *Plant J* 16: 735–743

Dreyfuss BW, Hamel PP, Nakamoto SS, Merchant S (2003) Functional analysis of a divergent system II protein, Ccs1, involved in *c*-type cytochrome biogenesis. *J Biol Chem* 278: 2604–2613

Endo T, Shikanai T, Sato F, Asada K (1998) NAD(P)H dehydrogenase-dependent, antimycin A-sensitive electron donation to plastoquinone in tobacco chloroplasts. *Plant Cell Physiol* 39: 1226–1231

Gupta R, He Z, Luan S (2002) Functional relationship of cytochrome c_6 and plastocyanin in *Arabidopsis*. *Nature* 417: 567–571

Hamel PP, Dreyfuss BW, Xie Z, Gabilly ST, Merchant S (2003) Essential histidine and tryptophan residues in CcsA, a system II polytopic cytochrome *c* biogenesis protein. *J Biol Chem* 278: 2593–2603

Konieczny A, Ausubel FM (1993) A procedure for mapping *Arabidopsis* mutations using co-dominant ecotype-specific PCR-based markers. *Plant J* 4: 403–410

Kramer DM, Johnson G, Kiirats O, Edwards GE (2004) New fluorescence parameters for the determination of Q_A redox state and excitation energy fluxes. *Photosynth Res* 79: 209–218

Kranz RG, Richard-Fogal C, Taylor JS, Frawley ER (2009) Cytochrome *c* biogenesis: mechanisms for covalent modifications and trafficking of heme and for heme-iron redox control. *Microbiol Mol Biol Rev* 73: 510–528

Krause GH, Weis E (1991) Chlorophyll fluorescence and photosynthesis: the basics. *Annu Rev Plant Physiol Plant Mol Biol* 42: 313–349

Kuras R, Saint-Marcoux D, Wollman FA, de Vitry C (2007) A specific *c*-type cytochrome maturation system is required for oxygenic photosynthesis. *Proc Natl Acad Sci USA* 104: 9906–9910

Kurisu G, Zhang H, Smith JL, Cramer WA (2003) Structure of the cytochrome b_6f complex of oxygenic photosynthesis: tuning the cavity. *Science* 302: 1009–1014

Ma J, Peng L, Guo J, Lu Q, Lu C, Zhang L (2007) LPA2 is required for efficient assembly of photosystem II in *Arabidopsis thaliana*. *Plant Cell* 19: 1980–1993

Miyake C, Asada K (1994) Ferredoxin-dependent photoreduction of monodehydroascorbate radicals in spinach thylakoids. *Plant Cell Physiol* 35: 539–549

Miyake C, Amako K, Shiraishi N, Sugimoto T (2009) Acclimation of *tobacco* leaves to high light intensity drives the plastoquinone oxidation system—relationship among the fraction of open PSII centers, non-photochemical quenching of Chl fluorescence and the maximum quantum yield of PSII in the dark. *Plant Cell Physiol* 50: 730–743

Munekage Y, Shikanai T (2005) Cyclic electron transport through photosystem I. *Plant Biotechnol* 22: 361–369

Munekage Y, Hojo M, Meurer J, Endo T, Tasaka M, Shikanai T (2002) PGR5 is involved in cyclic electron flow around photosystem I and is essential for photoprotection in *Arabidopsis*. *Cell* 110: 361–371

Munekage Y, Takeda S, Endo T, Jahns P, Hashimoto T, Shikanai T (2001) Cytochrome b_6f mutation specifically affects thermal dissipation of absorbed light energy in *Arabidopsis*. *Plant J* 28: 351–359

Munekage Y, Hashimoto M, Miyake C, Tomizawa K, Endo T, Tasaka M, Shikanai T (2004) Cyclic electron flow around photosystem I is essential for photosynthesis. *Nature* 429: 579–582

Okegawa Y, Kagawa Y, Kobayashi Y, Shikanai T (2008) Characterization of factors affecting the activity of photosystem I cyclic electron transport in chloroplasts. *Plant Cell Physiol* 49: 825–834

Okegawa Y, Tsuyama M, Kobayashi Y, Shikanai T (2005) The *pgr1* mutation in the Rieske subunit of the cytochrome b_6f complex does not affect PGR5-dependent cyclic electron transport around photosystem I. *J Biol Chem* 280: 28332–28336

Ozawa S, Nield J, Terao A, Stauber EJ, Hippler M, Koike H, Rochaix J-D, Takahashi Y (2009) Biochemical and structural studies of the large Ycf4-photosystem I assembly complex of the green alga *Chlamydomonas reinhardtii*. *Plant Cell* 21: 2424–2442

Peng L, Fukao Y, Fujiwara M, Takami T, Shikanai T (2009) Efficient operation of NAD(P)H dehydrogenase requires supercomplex formation with photosystem I via minor LHCI in *Arabidopsis*. *Plant Cell* 21: 3623–3640

Peng L, Ma J, Chi W, Guo J, Zhu S, Lu Q, Lu C, Zhang L (2006) LOW PSII ACCUMULATION1 is involved in efficient assembly of photosystem II in *Arabidopsis thaliana*. *Plant Cell* 18: 955–969

Rochaix J-D (2004) Genetics of the biogenesis and dynamics of the photosynthetic machinery in eukaryotes. *Plant Cell* 16: 1650–1660.

Schwenkert S, Legen J, Takami T, Shikanai T, Herrmann RG, Meurer J (2007) Role of the low-molecular-weight subunits PetL, PetG, and PetN in assembly, stability, and dimerization of the cytochrome b_6f complex in *tobacco*. *Plant Physiol* 144: 1924–1935

Shikanai T (2007) Cyclic electron transport around photosystem I: genetic approaches. *Annu Rev Plant Biol* 58: 199–217

Shikanai T, Müller-Moulé P, Munekage Y, Niyogi KK, Pilon M (2003) PAA1, a P-type ATPase of Arabidopsis, functions in copper transport in chloroplasts. *Plant Cell* 15: 1333–1346

Vargas C, McEwan AG, Downie JA (1993) Detection of c-type cytochromes using enhanced chemiluminescence. *Anal Biochem* 209: 323–326

Whitelegge JP, Zhang H, Aguilera R, Taylor RM, Cramer WA (2002) Full subunit coverage liquid chromatography electrospray ionization mass spectrometry (LCMS+) of an oligomeric membrane protein: cytochrome b_6f complex from *spinach* and the cyanobacterium *Mastigocladus laminosus*. *Mol Cell Proteomics* 1: 816–827

Wintz H, Vulpe C (2002) Plant copper chaperones. *Biochem Soc Trans* 30: 732–735

Wollman FA, Minai L, Nechushtai R (1999) The biogenesis and assembly of photosynthetic proteins in thylakoid membranes. *Biochim Biophys Acta* 1411: 21–85